

A Rainbow Structural-Color Chip for Multisaccharide Recognition

Meng Qin, Yu Huang, Yanan Li, Meng Su, Bingda Chen, Heng Sun, Peiyi Yong, Changqing Ye, Fengyu Li,* and Yanlin Song*

Abstract: A critical requirement for the successful recognition of multiple analytes is the acquisition of abundant sensing information. However, for this to be achieved requires massive chemical sensors or multiplex materials, which complicates the multianalysis. Thus, there is a need to develop a strategy for the facile and efficient recognition of multiple analytes. Herein, we explore the angle-dependent structural colors of photonic crystals to provide abundant optical information, thereby generating a rainbow-color chip to realize the convenient recognition of multiple analytes. By simply using a multiangle analysis method, the monophotonic crystal matrix chip can differentially enhance fluorescence signals over broad spectral ranges, thereby resulting in abundant sensing information for highly efficient multiple analysis. Twelve saccharides with similar structures, as well as saccharides in different concentrations and mixtures, were successfully discriminated.

The recognition of multiple analytes has drawn increased attention in the areas of clinical diagnosis,^[1] biological screening,^[2] the food industry,^[3] vapor monitoring,^[4] etc. A critical requirement for successful multiple recognition is the acquisition of abundant sensing information. In general, large numbers of sensing molecules or indicators have to be employed to attain sufficient sensing information, but this always involves complicated synthesis or massive screening programs.^[5] Selective signal enhancement by physical methods could provide an opportunity for increased sensing information to achieve facile and efficient recognition of multiple analytes, without the need for large numbers of chemical compounds. Photonic crystals (PCs) have been widely employed to facilitate the area of detection, mainly through structural colors,^[6] reflectance,^[7] and fluorescence enhancement^[8] induced by the unique photonic stop bands, which endow the platform with the desired abundant optical information. Although a PC chip with multiple stop bands could achieve successful multianalysis with a simple dye,^[9] the

fabrication and integration of multiplex PC materials matrix still remains a complex process.

As a class of periodic structured materials, PCs can control the propagation of light, which is characterized by an angle dependence.^[10] A PC matrix with a long-range-ordered structure can exhibit structural colors in consecutive spectra, reminiscent of a rainbow seen in nature. As shown in Figure 1a, a PC matrix film assembled from poly(styrene/methyl methacrylate/acrylic acid) [poly(St-MMA-AA)] latex particles with diameter of 270 nm exhibits a strong red color when illuminated with white light at normal incidence. When the film is rotated, which causes a simultaneous increase in the incident angle and reflection angle from 0° to 80°, the color changes from red to orange and finally to bluish violet. Thus, with various detection angles (referred to as the reflection angles, which are equal to the incident angles), a single PC matrix can serve as a platform to provide abundant optical information, and allow the facile construction of a sensor chip for the recognition of multiple analytes. Here, we combined the fluorescence enhancement properties of PCs with a single PC matrix film, fabricated by the self-assembly of poly(St-MMA-AA) latex particles (diameter of 270 nm),^[11] to develop a rainbow structural-color chip for the detection of multiple analytes. This flexible polymer chip can be used to differentially enhance fluorescence signals over broad spectral regions by simple application of a multiangle analysis method, thereby resulting in abundant sensing information for multiple analyses with high efficiency (Figure 1b).

Since the fluorescence enhancement properties of PCs are attributed to the slow photons effect at the stop band edges^[12] and emission reflection at the surface,^[13] the impact of detection angles on the location of stop bands and reflection intensity were investigated. As shown in Figure 1c, a simultaneous change in the incident angle and detection angle θ resulted in the experimental and theoretical values (calculated from Bragg's law and Snell's law^[14]) of the reflection peaks matching very well, thus indicating the high quality of the PC matrix film. Not only the location of stop bands but also the reflection intensity of the PC matrix film varies with the detection angles. As shown in Figure 1d, the reflectivity (expressed as the ratio of the reflection intensity at θ and 0°, R_θ/R_0) decreases as the angle increases. The reduced reflectivity may originate from increased scattering of random light by other crystal planes, as the baselines of the reflectance spectra increase as the angle increases (Figure S2).

To investigate the influences of detection angles on the fluorescence-enhancing capability, we tested the fluorescence of PC matrix films loaded with rhodamine B, fluorescein, and coumarin 314 (emissions at $\lambda = 594$ nm, 521 nm, and 480 nm, respectively) at detection angles (or incident angles) of 0°,

[*] M. Qin, Dr. Y. Huang, Y. Li, M. Su, B. Chen, H. Sun, P. Yong, Dr. C. Ye, Dr. F. Li, Prof. Y. Song
Key Laboratory of Green Printing
Institute of Chemistry, Chinese Academy of Sciences (ICCAS)
Beijing Engineering Research Center of Nanomaterials for Green
Printing Technology
Beijing National Laboratory for Molecular Sciences (BNLMS)
Beijing 100190 (P.R. China)
E-mail: forrest@iccas.ac.cn
ylsong@iccas.ac.cn

M. Qin, Y. Li, M. Su
University of Chinese Academy of Sciences
Beijing 100049 (P.R. China)

Supporting information for this article can be found under:
<http://dx.doi.org/10.1002/anie.201602582>.

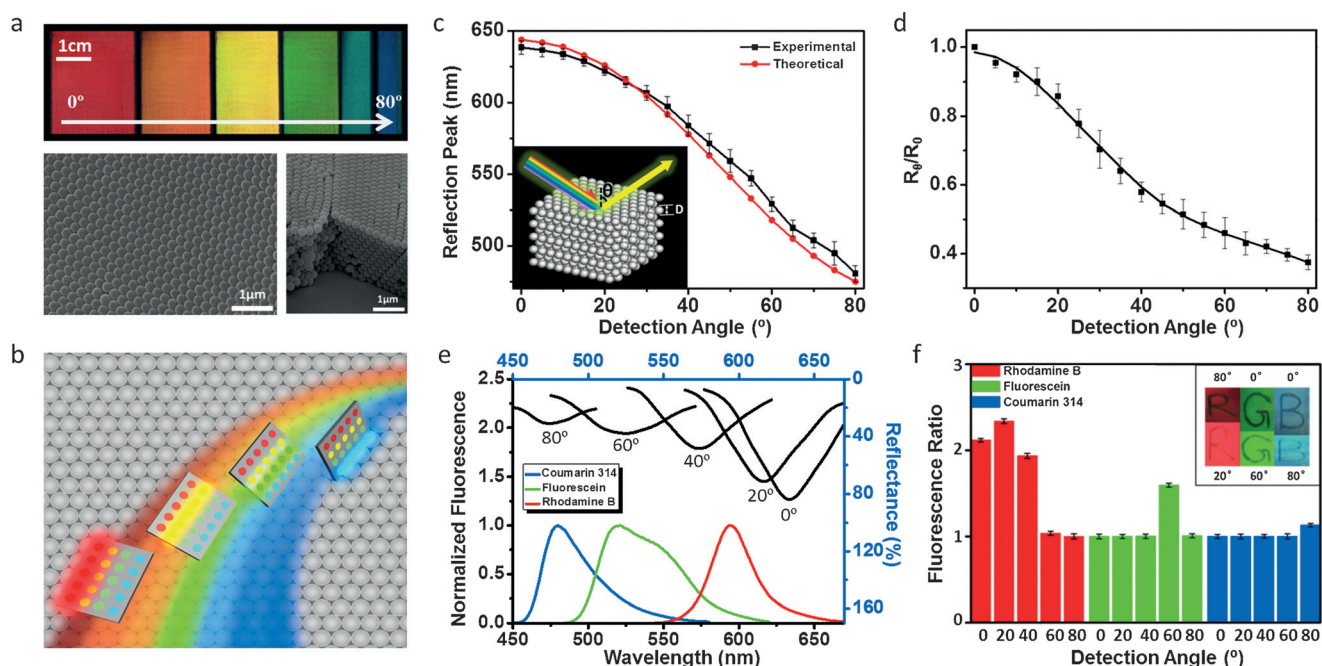


Figure 1. a) Photograph of a PC matrix film with viewing angles from 0° to 80° under illumination with white light (top) and the corresponding SEM images (bottom). The film exhibits structural colors in consecutive spectra, which are attributed to the long-range ordered arrangement of latex particles. b) Schematic illustration of the rainbow-color PC chip. The multiangle analysis method enables the PC chip to differentially enhance fluorescence signals over broad spectral regions. c) Experimental and theoretical values of the reflection peaks of the PC matrix film with increasing detection angles. The inset shows a simulation of light scattering on PCs. The high quality of the PC matrix film contributes to the well-matched experimental and calculated values. d) Changes in the reflection intensity upon increasing the detection angles. e) Fluorescence spectra of dyes and stop bands of the PC matrix film at detection angles of 0°, 20°, 40°, 60°, and 80°. f) Changes in the fluorescence of dyed PC matrix films upon increasing the detection angles. The inset shows the corresponding fluorescence images superimposed in three channels (CH1 $\lambda = 605$ nm, CH2 $\lambda = 535$ nm, and CH3 $\lambda = 450$ nm) at various detection angles. The PC matrix film is able to enhance the fluorescence in different spectral regions to a varying degree (rhodamine B “R”, fluorescein “G” and coumarin 314 “B”).

20°, 40°, 60°, and 80° (stop bands located at 634 nm, 617 nm, 573 nm, 526 nm, and 475 nm, respectively; Figure 1e). As shown in Figure 1f, different dyes exhibit distinct angle-based changes in the fluorescence (expressed as the ratio between the fluorescence intensity at θ and the minimum intensity). The fluorescence responses are collected from four randomly selected regions in the fluorescence images of dye-loaded PC matrix films (inset of Figure 1f). For the red fluorescent rhodamine B, the fluorescence is clearly enhanced at 0°, 20°, and 40°, since the band edges match the emission at $\lambda = 594$ nm. As a consequence of more overlap of band edges and stronger reflectivity, the PC matrix film at 20° displays the highest enhancing effect—2.3-fold more than at 80°. The green fluorescent fluorescein shows remarkable fluorescence intensity at 60°, because of the well-matched blue band edge and emission at $\lambda = 521$ nm. In the case of blue fluorescent coumarin 314, only the PC matrix film with a detection angle of 80° leads to relatively enhanced fluorescence, as the red band edge matches the emission at $\lambda = 480$ nm. The enhancing effect (1.1-fold higher than the minimum fluorescence intensity) is not as significant as that of the PC matrix film loaded with rhodamine B, because of the greatly decreased reflectivity. The PC matrix film exhibits selective fluorescence enhancement at different detection angles, since the effect of the slow photons and the emission reflection are altered

(details of the mechanism are discussed in the Supporting Information).

Since various detection angles endow a single PC matrix film with the ability to enhance the fluorescence in different spectral regions to varying degrees, the film can easily provide abundant fluorescence-based sensing signals. We used multi-angle analysis of saccharides on the PC matrix film to verify the novel facile recognition of multiple compounds by a simple material. As hydroxy groups are the only functional groups of saccharides and the structural differences of the saccharides are subtle apart from some steric diversity, it makes discrimination extremely tough.^[15] Here, we studied the recognition of 12 saccharides by simple ensembles containing a commercially available dye alizarin red-S (ARS), composited with phenylboronic acid (PBA) and diphenylborinic acid 2-aminoethyl ester (DPBA). ARS-PBA and ARS-DPBA show different fluorescence (emissions at $\lambda = 563$ nm and 590 nm, respectively), which can be selectively enhanced by the PC matrix film at different detection angles. After the addition of saccharides, the fluorescence will be changed because of the competitive binding of saccharides with PBA or DPBA (for details see the Supporting Information).^[16]

The PC matrix film was fabricated on a polyethylene terephthalate (PET) substrate and could be bent into

arbitrary radians with consecutive angle gradients (Figure 2a). After spotting with fluorescent ARS-PBA and ARS-DPBA complexes, the PC chip was used to recognize saccharides prepared in buffer solution (10 mM). As shown in Figure 2b (superimposition of fluorescence images in two channels: CH1 $\lambda = 605$ nm and CH2 $\lambda = 535$ nm), changes in the detection angle lead to diversity in the fluorescence signals. The fingerprint pattern becomes brighter from 0° to 30° , especially the fluorescence in the reddish orange spectral region. The ARS-DPBA responses to saccharides are strongly enhanced, as the blue band edge at 30° overlaps the emission at $\lambda = 590$ nm (Figure S4). At 45° , the reddish orange fluorescence reduces significantly, while the yellowish green ARS-PBA responses remain, because the reflection peak of the PC chip is located at $\lambda = 561$ nm and matches well the emission at $\lambda = 563$ nm. When the detection angle is 60° , the reddish orange signals continue to decrease, and the fluorescence remains predominantly in the greenish spectral region. Fluorescence results collected in each channel prove the selective fluorescence enhancement (Tables S4 and S5 and Figure S8). Thus, the PC chip provides abundant fluorescence signals in response to saccharides and enhances the differentials of the responses.

The identification of the saccharides by using linear discriminant analysis (LDA) on the data obtained to evaluate the similarities between data clusters^[17] is displayed in Figure 2c. F1 and F2 are the first two functions that describe the greatest spatial separation of the data.^[18] As shown by the score plots, 12 saccharides and 1 buffer control sample are discriminated successfully. Each detection angle contributes a discriminating capability of 75 % correct classification at 0° , 73 % at 30° , 67 % at 45° , and 75 % at 60° . Structurally similar saccharides are thus distinguished by the PC chip with only two sensing complexes. In contrast, a PET chip without a PC structure shows 87 % correct classification (Figure S6). Furthermore, we applied the PC chip to the recognition of analytes at different concentrations and in mixtures, which was necessary for practical applications but challenging because of cross-interference. Various impacts of the detection angles on the curves (concentrations versus fluorescence responses) help to give abundant sensing information for saccharides at different concentrations (Figure S9). As shown in Figure 2d, D-fructose, sucrose, and D-xylose are clearly separated at gradient concentrations (1 mM, 5 mM, 10 mM, 50 mM, 100 mM) by the cooperation of detection angles of 0° , 30° , 45° , and 60° . The distribution of the clusters is scattered

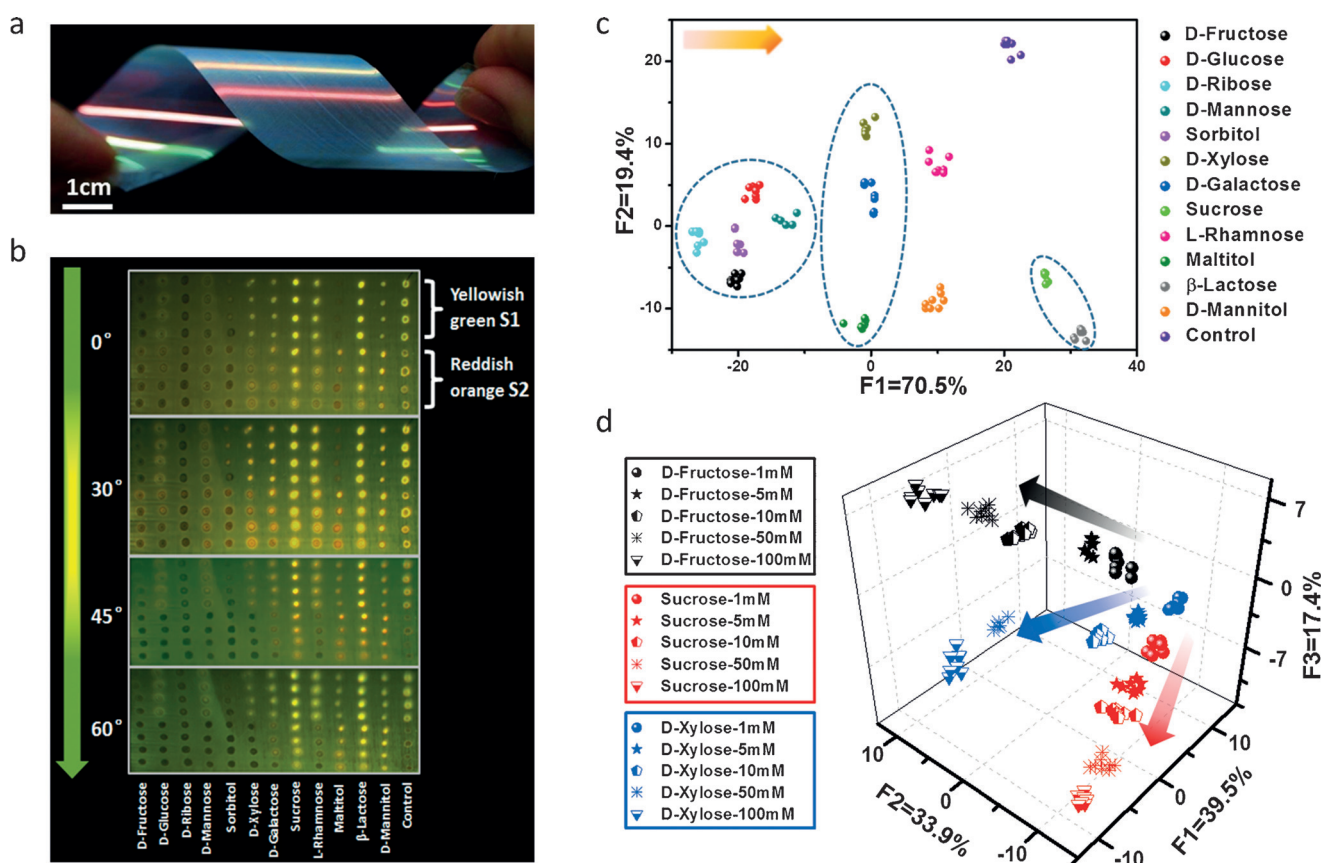


Figure 2. Rainforest-color PC chip for identification of saccharides. a) Photograph of the flexible PC matrix film with a distribution of rainbow colors. b) Fluorescence responses of a PC chip spotted with ARS-PBA (S1, yellowish green) and ARS-DPBA (S2, reddish orange) to 12 saccharides and 1 buffer control sample. The changes in the detection angle lead to diversity in the fluorescence signals. c) LDA results in the discrimination of 12 saccharides. F1 and F2 are the first two functions that describe the greatest spatial separation of the data. The arrow indicates an increase in the fluorescence. d) Score plots of saccharides in gradient concentrations. The distribution of the clusters is scattered along the increased concentrations indicated by the arrows. F1–F3 are the first three functions that determine the greatest spatial separation of the data.

along the increased concentrations, which coincides with the remarkable fluorescence contrast induced by the larger concentration (Figure S10). Furthermore, mixtures can be successfully recognized (Figure S11). The results reveal the powerful sensing capabilities of the PC chip.

In conclusion, a rainbow structural-color PC chip was explored to provide abundant optical information, and achieve facile recognition of multiple saccharides. Multiangle analysis was proposed as a substitute for massive chemical sensors and multiplex PC materials. The blue-shifted location of the photonic stop bands as the detection angles of a single PC matrix chip increases, indicates the enhancement capability for fluorescence over broad spectral regions, and the reduced reflection intensity suggests the enhancement occurs to a varying degree. By simply employing a multiangle analysis method, the PC chip can differentially enhance fluorescence signals in various spectral regions, thus providing sufficient sensing information for high-efficiency multianalysis. The PC chip can facilitate discriminate 12 similarly structured saccharides. Furthermore, it is possible to distinguish saccharides at different concentrations and in mixtures. The sensing strategy based on a rainbow-color PC chip avoids the need for a complicated design and screening of sensing elements, thereby providing a new method to perform high-efficiency multianalysis. The strategy to achieve flexible and printable multianalyte chips will be of significance for the development of wearable sensing devices.

Acknowledgements

We thank 973 Program (Nos. 2013CB933004), the National Nature Science Foundation (Grant Nos. 51203166, 51473172, 51473173), and the “Strategic Priority Research Program” of the Chinese Academy of Sciences (Grant No. XDA09020000) for financial support.

Keywords: Analytical methods · multianalyte · photonic crystals · sensors · structural color

How to cite: *Angew. Chem. Int. Ed.* **2016**, *55*, 6911–6914
Angew. Chem. **2016**, *128*, 7025–7028

- [1] N. Kahn, O. Lavie, M. Paz, Y. Segev, H. Haick, *Nano Lett.* **2015**, *15*, 7023–7028.
- [2] M. Qin, F. Li, Y. Huang, W. Ran, D. Han, Y. Song, *Anal. Chem.* **2015**, *87*, 837–842.
- [3] A. P. Umali, S. E. LeBoeuf, R. W. Newberry, S. Kim, L. Tran, W. A. Rome, T. Tian, D. Taing, J. Hong, M. Kwan, H. Heymann, E. V. Anslyn, *Chem. Sci.* **2011**, *2*, 439–445.
- [4] H. Lin, M. Jang, K. S. Suslick, *J. Am. Chem. Soc.* **2011**, *133*, 16786–16789.
- [5] a) Y. Liu, T. Minami, R. Nishiyabu, Z. Wang, P. Anzenbacher, *J. Am. Chem. Soc.* **2013**, *135*, 7705–7712; b) X. Zhang, L. You, E. V. Anslyn, X. Qian, *Chem. Eur. J.* **2012**, *18*, 1102–1110.
- [6] a) Y. Zhang, Q. Fu, J. Ge, *Nat. Commun.* **2015**, *6*, 7510; b) Z. Cai, D. H. Kwak, D. Punihale, Z. Hong, S. S. Velankar, X. Liu, S. A. Asher, *Angew. Chem. Int. Ed.* **2015**, *54*, 13036–13040; *Angew. Chem.* **2015**, *127*, 13228–13232; c) J.-P. Couturier, M. Sütterlin, A. Laschewsky, C. Hettrich, E. Wischerhoff, *Angew. Chem. Int. Ed.* **2015**, *54*, 6641–6644; *Angew. Chem.* **2015**, *127*, 6741–6745; d) J.-W. Oh, W.-J. Chung, K. Heo, H.-E. Jin, B. Y. Lee, E. Wang, C. Zueger, W. Wong, J. Meyer, C. Kim, S.-Y. Lee, W.-G. Kim, M. Zemla, M. Auer, A. Hexemer, S.-W. Lee, *Nat. Commun.* **2014**, *5*, 3043; e) C. Fenzl, T. Hirsch, O. S. Wolfbeis, *Angew. Chem. Int. Ed.* **2014**, *53*, 3318–3335; *Angew. Chem.* **2014**, *126*, 3384–3402; f) J. Cui, W. Zhu, N. Gao, J. Li, H. Yang, Y. Jiang, P. Seidel, B. J. Ravoo, G. Li, *Angew. Chem. Int. Ed.* **2014**, *53*, 3844–3848; *Angew. Chem.* **2014**, *126*, 3923–3927; g) Z. Xie, K. Cao, Y. Zhao, L. Bai, H. Gu, H. Xu, Z.-Z. Gu, *Adv. Mater.* **2014**, *26*, 2413–2418; h) K. I. MacConaghay, C. I. Geary, J. L. Kaar, M. P. Stoykovich, *J. Am. Chem. Soc.* **2014**, *136*, 6896–6899; i) J. Ge, Y. Yin, *Angew. Chem. Int. Ed.* **2011**, *50*, 1492–1522; *Angew. Chem.* **2011**, *123*, 1530–1561.
- [7] R. A. Potyrailo, R. K. Bonam, J. G. Hartley, T. A. Starkey, P. Vukusic, M. Vasudev, T. Bunning, R. R. Naik, Z. Tang, M. A. Palacios, M. Larsen, L. A. Le Tarte, J. C. Grande, S. Zhong, T. Deng, *Nat. Commun.* **2015**, *6*, 7959.
- [8] a) J. Hou, H. Zhang, Q. Yang, M. Li, Y. Song, L. Jiang, *Angew. Chem. Int. Ed.* **2014**, *53*, 5791–5795; *Angew. Chem.* **2014**, *126*, 5901–5905; b) M. Li, F. He, Q. Liao, J. Liu, L. Xu, L. Jiang, Y. Song, S. Wang, D. Zhu, *Angew. Chem. Int. Ed.* **2008**, *47*, 7258–7262; *Angew. Chem.* **2008**, *120*, 7368–7372.
- [9] Y. Huang, F. Li, M. Qin, L. Jiang, Y. Song, *Angew. Chem. Int. Ed.* **2013**, *52*, 7296–7299; *Angew. Chem.* **2013**, *125*, 7437–7440.
- [10] a) J. I. L. Chen, G. von Freymann, S. Y. Choi, V. Kitaev, G. A. Ozin, *Adv. Mater.* **2006**, *18*, 1915–1919; b) P. Lodahl, A. Floris van Driel, I. S. Nikolaev, A. Irman, K. Overgaag, D. Vanmaekelbergh, W. L. Vos, *Nature* **2004**, *430*, 654–657.
- [11] J. Wang, Y. Wen, H. Ge, Z. Sun, Y. Zheng, Y. Song, L. Jiang, *Macromol. Chem. Phys.* **2006**, *207*, 596–604.
- [12] a) J. I. L. Chen, G. von Freymann, S. Y. Choi, V. Kitaev, G. A. Ozin, *J. Mater. Chem.* **2008**, *18*, 369–373; b) K. Yoshino, S. B. Lee, S. Tatsuhara, Y. Kawagishi, M. Ozaki, A. A. Zakhidov, *Appl. Phys. Lett.* **1998**, *73*, 3506–3508.
- [13] Y.-Q. Zhang, J.-X. Wang, Z.-Y. Ji, W.-P. Hu, L. Jiang, Y.-L. Song, D.-B. Zhu, *J. Mater. Chem.* **2007**, *17*, 90–94.
- [14] a) A. Richel, N. P. Johnson, D. W. McComb, *Appl. Phys. Lett.* **2000**, *76*, 1816–1818; b) T. Yamasaki, T. Tsutsui, *Appl. Phys. Lett.* **1998**, *72*, 1957–1959.
- [15] a) X. Wu, Z. Li, X.-X. Chen, J. S. Fossey, T. D. James, Y.-B. Jiang, *Chem. Soc. Rev.* **2013**, *42*, 8032–8048; b) C. J. Musto, S. H. Lim, K. S. Suslick, *Anal. Chem.* **2009**, *81*, 6526–6533; c) J. W. Lee, J.-S. Lee, Y.-T. Chang, *Angew. Chem. Int. Ed.* **2006**, *45*, 6485–6487; *Angew. Chem.* **2006**, *118*, 6635–6637; d) P. Chen, M. T. Chung, W. McHugh, R. Nidetz, Y. Li, J. Fu, T. T. Cornell, T. P. Shanley, K. Kurabayashi, *ACS Nano* **2015**, *9*, 4173–4181.
- [16] G. Springsteen, B. Wang, *Chem. Commun.* **2001**, 1608–1609.
- [17] S. Stewart, M. A. Ivy, E. V. Anslyn, *Chem. Soc. Rev.* **2014**, *43*, 70–84.
- [18] N. Y. Edwards, T. W. Sager, J. T. McDevitt, E. V. Anslyn, *J. Am. Chem. Soc.* **2007**, *129*, 13575–13583.

Received: March 14, 2016

Published online: April 26, 2016